Vietnam Journal of Mechanics, VAST, Vol. 44, No. 1 (2022), pp. 15 – 28
DOI: https://doi.org/10.15625/0866-7136/16575

NONLINEAR RESPONSE OF DOUBLY CURVED SANDWICH PANELS WITH CNT-REINFORCED COMPOSITE CORE AND ELASTICALLY RESTRAINED EDGES SUBJECTED TO EXTERNAL PRESSURE IN THERMAL ENVIRONMENTS

Hoang Van Tung[1,*], **Dao Nhu Mai**[2], **Vu Thanh Long**[3]
[1]*Faculty of Civil Engineering, Hanoi Architectural University, Hanoi, Vietnam*
[2]*Institute of Mechanics, VAST, 18 Hoang Quoc Viet street, Cau Giay district, Hanoi, Vietnam*
[3]*Faculty of Civil Engineering, University of Transport Technology, Hanoi, Vietnam*
[*]E-mail: tunghv@hau.edu.vn

Received: 25 September 2021 / Published online: 11 December 2021

Abstract. An analytical investigation on the nonlinear response of doubly curved panels constructed from homogeneous face sheets and carbon nanotube reinforced composite (CNTRC) core and subjected to external pressure in thermal environments is presented in this paper. Carbon nanotubes (CNTs) are reinforced into the core layer through uniform or functionally graded distributions. The properties of constituents are assumed to be temperature dependent and effective properties of CNTRC are determined using an extended rule of mixture. Governing equations are established within the framework of first order shear deformation theory taking into account geometrical imperfection, von Kármán–Donnell nonlinearity, panel-foundation interaction and elasticity of tangential edge restraints. These equations are solved using approximate analytical solutions and Galerkin method for simply supported panels. The results reveal that load carrying capacity of sandwich panels is stronger when boundary edges are more rigorously restrained and face sheets are thicker. Furthermore, elevated temperature has deteriorative and beneficial influences on the load bearing capability of sandwich panels with movable and restrained edges, respectively.

Keywords: doubly curved panel, FG-CNTRC, sandwich shell, tangential edge restraint, thermomechanical load.

1. INTRODUCTION

Due to superior properties such as extremely high stiffness and strength together with very large aspect ratio, carbon nanotubes (CNTs) are ideal fillers into isotropic matrix to form carbon nanotube reinforced composite (CNTRC), a new class of advanced nanocomposite [1, 2]. The idea of optimal distribution of CNTs motivates the concept of functionally graded carbon nanotube reinforced composite (FG-CNTRC) [3] in which

CNTs are embedded into the matrix in such a way that their volume is varied in the thickness direction of structure according to functional rules. Shen's propositional work [3] stimulated subsequent investigations on the static and dynamic responses of FG-CNTRC structures [4–13]. Based on a higher order shear deformation theory (HSDT) and a two-step perturbation approach, Shen and coworkers [14–16] investigated the postbuckling of pressure-loaded doubly curved panels made of functionally graded (FG) material, CNTRC and graphene-reinforced composite (GRC). In these studies, the effects of elastic foundations, initial imperfection and thermal environments on the postbuckling of pressure-loaded doubly curved panels have been taken into consideration.

Sandwich-type structures possess many outstanding characteristics such as very high ratio of stiffness to weight and excellent sound dissolution. Accordingly, sandwich components in forms of beams, plates and shells are widely used in structural applications, especially in aerospace engineering. The generation of advanced composites such as CNTRC necessitates insight of static and dynamic responses of sandwich structures composed of CNTRC. Using a HSDT and asymptotic solutions, Shen and Zhu [17] explored the postbuckling behavior of sandwich plates with CNTRC face sheets under thermal and compressive loads. A postbuckling analysis of sandwich plates with CNTRC face sheets and various boundary conditions under uniform temperature rise has been carried out by Kiani [18] utilizing Chebyshev–Ritz method and first order shear deformation theory (FSDT). Basing on a finite element approach, Mehar and coworkers [19–21] presented numerical investigations on linear flexural, vibration and buckling behaviors of FG-CNTRC sandwich curved panels subjected to thermal loadings. The supersonic flutter characteristics of thick doubly curved sandwich panels with CNTRC face sheets were examined in work of Sankar et al. [22] employing higher order structural theory and finite element method. A semi-analytical method was used in study of Wang et al. [23] to analyze the linear vibration of sandwich plates with CNTRC face sheets. In aforementioned works, sandwich plates and shells are composed of homogeneous core layer and CNTRC face sheets. According to standard model of sandwich structure, core layer should be thicker and lighter, whereas face sheets should be thinner and stiffer. Towards this standard sandwich model, beside sandwich structure considered in above works [17–23], a new sandwich model with CNTRC core layer and homogeneous face sheets has been suggested in works of Long and Tung [24–26]. These works studied the postbuckling behaviors of sandwich rectangular plates and cylindrical panels with FG-CNTRC face sheets or core layer under compressive, thermal and thermomechanical loads. Subsequently, Hieu and Tung [27] treated the linear buckling problem of sandwich cylindrical shells constructed from FG-CNTRC and homogeneous layers subjected to uniform temperature rise and external pressure. Previous studies [24–27] revealed that efficiencies of buckling resistance and load carrying in postbuckling region can be optimal when sandwich structures are made of thicker CNTRC core layer and thin homogeneous face sheets. Recently, Forountan et al. [28] used a semi-analytical method for static and dynamic postbuckling analyses of sandwich cylindrical panels with an FG-CNTRC core resting on nonlinear viscoelastic foundations.

As an extension of previous works [9, 10], this paper aims to analyze the effects of tangential edge constrains, preexisting thermal environments and elastic foundations on the nonlinear stability response of doubly curved sandwich panels with FG-CNTRC core layer subjected to uniform external pressure. Formulations are based on the first order shear deformation theory taking into account geometrical imperfection, von Kármán–Donnell nonlinearity and interactive pressure from elastic foundations. Approximate analytical solutions and Galerkin method are adopted to solve basic equations and obtain closed-form result of load-deflection relation. Parametric studies are carried out to evaluate different influences on the load carrying capacity of sandwich panels.

2. MATERIAL AND STRUCTURAL MODELS

As shown in Fig. 1, structural model considered in this study is a doubly curved sandwich panel of planar dimensions a, b, total thickness h and curvature radii R_x, R_y in the directions a, b, respectively. It is assumed that panel is relatively shallow, viz planar dimensions a, b are much smaller than curvature radii R_x, R_y. The panel is rested on a two-parameter elastic foundation and defined in a coordinate system xyz the origin of which is located on the middle surface at one corner, x and y axes are directed toward a and b, respectively, and z is in the direction of inward normal to the middle surface. The panel is constituted from homogeneous face sheets and CNTRC core in which CNTs are aligned in the direction of x axis. It is assumed that core layer and face sheets are perfectly bonded and thickness of each face sheet is h_f.

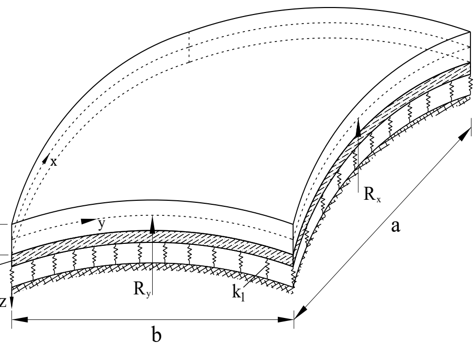

Fig. 1. Configuration and coordinate system of a doubly curved panel on an elastic foundation

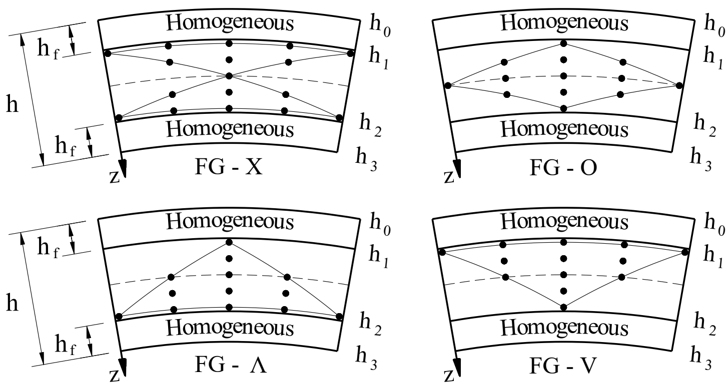

Fig. 2. Functionally graded (FG) patterns of CNT distribution in core layer of sandwich panel

CNTs are reinforced into core layer according to uniform distribution (UD) or functionally graded (FG) distribution patterns named FG-X, FG-O, FG-Λ and FG-V as illustrated in Fig. 2.

The volume fraction V_{CNT} of CNTs corresponding to these distributions are given as follows

$$V_{CNT} = \begin{cases} V^*_{CNT} & \text{UD} \\ 4\dfrac{|z|}{h_2 - h_1} V^*_{CNT} & \text{FG-X} \\ 2\dfrac{z - h_1}{h_2 - h_1} V^*_{CNT} & \text{FG-}\Lambda \\ 2\dfrac{h_2 - z}{h_2 - h_1} V^*_{CNT} & \text{FG-V} \\ 2\left(1 - \dfrac{2\,|z|}{h_2 - h_1}\right) V^*_{CNT} & \text{FG-O} \end{cases} \tag{1}$$

in which $h_1 = -h/2 + h_f$,$h_2 = h/2 - h_f$ and V^*_{CNT} is total volume fraction of CNTs. The volume fraction of matrix material in CNTRC core layer is $V_m = 1 - V_{CNT}$. In practice, CNTs usually curved and agglomerative. In this study, CNTs are assumed to be straight and aligned. Based on a micromechanical approach, the effective elastic moduli E_{11}, E_{22} and effective shear modulus G_{12} of CNTRC are determined according to an extended rule of mixture as [3]

$$E_{11} = \eta_1 V_{CNT} E^{CNT}_{11} + V_m E^m, \tag{2a}$$

$$\frac{\eta_2}{E_{22}} = \frac{V_{CNT}}{E^{CNT}_{22}} + \frac{V_m}{E^m}, \tag{2b}$$

$$\frac{\eta_3}{G_{12}} = \frac{V_{CNT}}{G^{CNT}_{12}} + \frac{V_m}{G^m}, \tag{2c}$$

where $E^{CNT}_{11}, E^{CNT}_{22}$ and G^{CNT}_{12} are elastic moduli and shear modulus of CNTs, respectively, whereas E^m and G^m are elastic and shear moduli of isotropic matrix material, respectively. In addition, η_1, η_2, η_3 are CNT efficiency parameters including size-dependent effects.

The effective Poisson's ratio of CNTRC is assumed to be constant and determined as [3]

$$\nu_{12} = V^*_{CNT} \nu^{CNT}_{12} + \left(1 - V^*_{CNT}\right) \nu^m, \tag{3}$$

in which ν^{CNT}_{12} and ν^m are Poisson's ratios of CNT and matrix material, respectively.

The effective coefficients of thermal expansion α_{11} and α_{22} in the longitudinal and transverse directions, respectively, are evaluated according to Schapery model as [18]

$$\alpha_{11} = \frac{V_{CNT} E^{CNT}_{11} \alpha^{CNT}_{11} + V_m E^m \alpha^m}{V_{CNT} E^{CNT}_{11} + V_m E^m}, \tag{4a}$$

$$\alpha_{22} = \left(1 + \nu^{CNT}_{12}\right) V_{CNT} \alpha^{CNT}_{22} + \left(1 + \nu^m\right) V_m \alpha^m - \nu_{12} \alpha_{11}, \tag{4b}$$

in which $\alpha^{CNT}_{11}, \alpha^{CNT}_{22}$ and α^m are thermal expansion coefficients of CNT and matrix material, respectively.

3. BASIC EQUATIONS

The sandwich panels are assumed to be moderately thick and basic equations are established within the framework of the first order shear deformation theory (FSDT). Based on the FSDT, strains at a distance z from the middle surface are expressed as [29]

$$\begin{pmatrix} \varepsilon_x \\ \varepsilon_y \\ \gamma_{xy} \end{pmatrix} = \begin{pmatrix} \varepsilon_x^0 \\ \varepsilon_y^0 \\ \gamma_{xy}^0 \end{pmatrix} + z \begin{pmatrix} \varepsilon_x^1 \\ \varepsilon_y^1 \\ \gamma_{xy}^1 \end{pmatrix}, \quad \begin{pmatrix} \gamma_{xz} \\ \gamma_{yz} \end{pmatrix} = \begin{pmatrix} \phi_x + w_{,x} \\ \phi_y + w_{,y} \end{pmatrix}, \tag{5}$$

where

$$\begin{pmatrix} \varepsilon_x^0 \\ \varepsilon_y^0 \\ \gamma_{xy}^0 \end{pmatrix} = \begin{pmatrix} u_{,x} - w/R_x + w_{,x}^2/2 \\ v_{,y} - w/R_y + w_{,y}^2/2 \\ u_{,y} + v_{,x} + w_{,x}w_{,y} \end{pmatrix}, \quad \begin{pmatrix} \varepsilon_x^1 \\ \varepsilon_y^1 \\ \gamma_{xy}^1 \end{pmatrix} = \begin{pmatrix} \phi_{x,x} \\ \phi_{y,y} \\ \phi_{x,y} + \phi_{y,x} \end{pmatrix}, \tag{6}$$

in which u, v, w are displacements of a point on the middle surface in the x, y, z directions, respectively, and ϕ_x, ϕ_y are rotations of a normal to the middle surface with respect to y, x axes, respectively.

Stress components in the sandwich panel are determined using constitutive relations as [29]

$$\begin{pmatrix} \sigma_x \\ \sigma_y \\ \sigma_{xy} \\ \sigma_{xz} \\ \sigma_{yz} \end{pmatrix} = \begin{pmatrix} Q_{11} & Q_{12} & 0 & 0 & 0 \\ Q_{12} & Q_{22} & 0 & 0 & 0 \\ 0 & 0 & Q_{66} & 0 & 0 \\ 0 & 0 & 0 & Q_{44} & 0 \\ 0 & 0 & 0 & 0 & Q_{55} \end{pmatrix} \begin{pmatrix} \varepsilon_x - \alpha_{11}\Delta T \\ \varepsilon_y - \alpha_{22}\Delta T \\ \gamma_{xy} \\ \gamma_{xz} \\ \gamma_{yz} \end{pmatrix}, \tag{7}$$

where $\Delta T = T - T_0$ is uniform temperature rise from room temperature T_0 and

$$Q_{11} = \frac{E_{11}}{1-\nu_{12}\nu_{21}}, Q_{22} = \frac{E_{22}}{1-\nu_{12}\nu_{21}}, Q_{12} = \frac{\nu_{21}E_{11}}{1-\nu_{12}\nu_{21}}, Q_{44} = G_{13}, Q_{55} = G_{23}, Q_{66} = G_{12}, \tag{8}$$

for CNTRC core layer, and

$$\begin{aligned} &E_{11} = E_{22} = E_H, \quad \alpha_{11} = \alpha_{22} = \alpha_H, \quad \nu_{12} = \nu_{21} = \nu_H, \\ &Q_{11} = Q_{22} = \frac{E_H}{1-\nu_H^2}, \quad Q_{12} = \frac{\nu_H E_H}{1-\nu_H^2}, \quad Q_{44} = Q_{55} = Q_{66} = \frac{E_H}{2(1+\nu_H)}, \end{aligned} \tag{9}$$

for face sheets in which E_H, α_H and ν_H denote the elastic modulus, thermal expansion coefficient and Poisson ratio of isotropic homogeneous material in the face sheets, respectively.

Force and moment resultants are calculated through stress components as follows

$$\begin{aligned} &(N_x, M_x) = (e_{11}, e_{12})\,\varepsilon_x^0 + \nu_{21}\,(e_{11}, e_{12})\,\varepsilon_y^0 + (e_{12}, e_{13})\,\phi_{x,x} + \nu_{21}\,(e_{12}, e_{13})\,\phi_{y,y} - (e_{11T}, e_{12T})\,\Delta T, \\ &(N_y, M_y) = \nu_{12}\,(e_{21}, e_{22})\,\varepsilon_x^0 + (e_{21}, e_{22})\,\varepsilon_y^0 + \nu_{12}\,(e_{22}, e_{23})\,\phi_{x,x} + (e_{22}, e_{23})\,\phi_{y,y} - (e_{21T}, e_{22T})\,\Delta T, \\ &(N_{xy}, M_{xy}) = (e_{31}, e_{32})\,\gamma_{xy}^0 + (e_{32}, e_{33})\,(\phi_{x,y} + \phi_{y,x}), \\ &Q_x = K_S e_{41}\,(\phi_x + w_{,x}), \quad Q_y = K_S e_{51}\,(\phi_y + w_{,y}), \end{aligned} \tag{10}$$

where

$$
\begin{aligned}
&(e_{11}, e_{21}, e_{31}, e_{41}, e_{51}) = \int\limits_{-h/2}^{h/2} (Q_{11}, Q_{22}, Q_{66}, Q_{44}, Q_{55})\, \mathrm{d}z, \\
&(e_{12}, e_{22}, e_{32}) = \int\limits_{-h/2}^{h/2} (Q_{11}, Q_{22}, Q_{66})\, z\mathrm{d}z, \quad (e_{13}, e_{23}, e_{33}) = \int\limits_{-h/2}^{h/2} (Q_{11}, Q_{22}, Q_{66})\, z^2\mathrm{d}z, \\
&(e_{11T}, e_{12T}) = \int\limits_{-h/2}^{h/2} Q_{11} (\alpha_{11} + \nu_{21}\alpha_{22}) (1, z)\, \mathrm{d}z, \quad (e_{21T}, e_{22T}) = \int\limits_{-h/2}^{h/2} Q_{22} (\nu_{12}\alpha_{11} + \alpha_{22}) (1, z)\, \mathrm{d}z,
\end{aligned} \tag{11}
$$

and K_S is shear correction coefficient.

Nonlinear equilibrium equation of doubly curved sandwich panels can be established based on mathematical procedure described in the works [8, 10] as follows

$$
\begin{aligned}
&a_{11}\phi_{x,xxx} + a_{21}\phi_{x,xyy} + a_{31}\phi_{y,xxy} + a_{41}\phi_{y,yyy} + a_{51}f_{,xxyy} + f_{,yy}\left(w_{,xx} + w^*_{,xx}\right) \\
&- 2f_{,xy}\left(w_{,xy} + w^*_{,xy}\right) + f_{,xx}\left(w_{,yy} + w^*_{,yy}\right) + \frac{f_{,yy}}{R_x} + \frac{f_{,xx}}{R_y} + q - k_1 w + k_2\left(w_{,xx} + w_{,yy}\right) = 0,
\end{aligned} \tag{12}
$$

in which $f(x, y)$ is a stress function defined as $N_x = f_{,yy}$, $N_y = f_{,xx}$, $N_{xy} = -f_{,xy}$, $w^*(x, y)$ is a known function representing initial geometrical imperfection, q is external pressure uniformly distributed on the outer surface of the panel, k_1 and k_2 are stiffness parameters of elastic and shear layers of Winkler–Pasternak foundation, respectively, and coefficients a_{j1} ($j = 1 \div 5$) are similar to those given in the work [24].

Strain compatibility equation of doubly curved sandwich panels can be derived by means of manner described in the works [8, 10] as follows

$$
\begin{aligned}
&a_{12}f_{,xxxx} + a_{22}f_{,xxyy} + a_{32}f_{,yyyy} + a_{42}\phi_{x,xxx} + a_{52}\phi_{y,xxy} + a_{62}\phi_{y,yyy} + a_{72}\phi_{x,xyy} \\
&- w^2_{,xy} + w_{,xx}w_{,yy} - 2w_{,xy}w^*_{,xy} + w_{,xx}w^*_{,yy} + w_{,yy}w^*_{,xx} + \frac{w_{,yy}}{R_x} + \frac{w_{,xx}}{R_y} = 0,
\end{aligned} \tag{13}
$$

where coefficients a_{k2} ($k = 1 \div 7$) can be found in the work [24].

In this work, all edges of the panel are assumed to be simply supported and tangentially restrained. The associated boundary conditions are expressed as follows [10, 29]

$$
w = \phi_y = M_x = 0, N_x = N_{x0} \quad \text{at} \quad x = 0, a \tag{14a}
$$

$$
w = \phi_x = M_y = 0, N_y = N_{y0} \quad \text{at} \quad y = 0, b \tag{14b}
$$

where N_{x0} and N_{y0} are fictitious force resultants at restrained edges and related to average end-shortening displacements at these edges as follows [8, 10]

$$
N_{x0} = -\frac{c_1}{ab}\int\limits_0^a\int\limits_0^b \frac{\partial u}{\partial x}\mathrm{d}y\mathrm{d}x, \quad N_{y0} = -\frac{c_2}{ab}\int\limits_0^a\int\limits_0^b \frac{\partial v}{\partial y}\mathrm{d}y\mathrm{d}x, \tag{15}
$$

in which c_1 and c_2 are stiffness parameters of tangential constraints at edges $x = 0, a$ and $y = 0, b$, respectively.

4. SOLUTION PROCEDURE

To satisfy boundary conditions (14), analytical solutions are assumed as follows [10]

$$(w, w^*) = (W, \mu h) \sin \beta_m x \sin \delta_n y, \tag{16a}$$

$$f = A_1 \cos 2\beta_m x + A_2 \cos 2\delta_n y + A_3 \sin \beta_m x \sin \delta_n y + \frac{1}{2} N_{x0} y^2 + \frac{1}{2} N_{y0} x^2, \tag{16b}$$

$$\phi_x = B_1 \cos \beta_m x \sin \delta_n y, \quad \phi_y = B_2 \sin \beta_m x \cos \delta_n y, \tag{16c}$$

where $\beta_m = m\pi/a$, $\delta_n = n\pi/b$ $(m, n = 1, 2, ...)$, W and μ are the amplitude of the deflection and size of imperfection, respectively, and A_i $(i = 1 \div 3)$, $B_j (j = 1, 2)$ are coefficients to be determined. These solutions are based on point of view that shape of deflection is developed from linear state (small deflection) through nonlinear state (large deflection). By substituting the solutions (16) into the compatibility equation (13), we obtain A_1, A_2 and an algebraic equation in terms of A_3, B_1 and B_2. After that, by introducing the solutions (16) into two equilibrium equations concerning shear forces as performed in the previous works [8, 10], we obtain a system of two algebraic equations in terms of A_3, B_1 and B_2. Lastly, solving the algebraic equations yields the following results

$$A_1 = \frac{\delta_n^2 W}{32 a_{12} \beta_m^2} (W + 2\mu h), \ A_2 = \frac{\beta_m^2 W}{32 a_{32} \delta_n^2} (W + 2\mu h), \ A_3 = A_3^* W, \ \ B_1 = B_1^* W, \ B_2 = B_2^* W, \tag{17}$$

in which specific expressions of A_3^*, B_1^* and B_2^* can be found in the work [10].

Next, fictitious force resultants N_{x0}, N_{y0} can be determined. Indeed, from relations (6) and (10) we can express $\partial u / \partial x$ and $\partial v / \partial y$ in terms of partial derivatives of deflection w, stress function f and rotations ϕ_x, ϕ_y. Then, by substituting the solutions (16) into the obtained expressions of $\partial u / \partial x$, $\partial v / \partial y$ and putting the resulting into the equations (15), we can obtain the fictitious force resultants N_{x0}, N_{y0} at tangentially restrained edges. However, these specific expressions are omitted here for the sake of brevity.

Now, introducing the solutions (16) into the equilibrium equation (12) and applying Galerkin method to the obtained equation lead to the following expression

$$q = b_1 \overline{W} + b_2 \overline{W} (\overline{W} + \mu) + b_3 \overline{W} (\overline{W} + 2\mu) + b_4 \overline{W} (\overline{W} + \mu)(\overline{W} + 2\mu) + b_5 (\overline{W} + \mu) \Delta T - b_6 \Delta T, \tag{18}$$

in which the form of coefficients b_k $(k = 1 \div 6)$ is similar to that given in the work [10]. This expression is nonlinear relation between load and deflection of doubly curved sandwich panels resting on elastic foundations and subjected to uniform external pressure in thermal environments.

5. NUMERICAL RESULTS AND DISCUSSION

This section presents numerical results for nonlinear response analysis of spherical and cylindrical sandwich panels with square platform $(a = b)$ constructed from homogeneous face sheets and CNTRC core layer. The homogeneous core is made of Ti-6Al-4V the temperature dependent properties of which are [18]

$$\begin{aligned} E_H &= 122.56 \left(1 - 4.586 \times 10^{-4} T\right) \text{GPa}, \\ \alpha_H &= 7.5788 \left(1 + 6.638 \times 10^{-4} T - 3.147 \times 10^{-7} T^2\right) \times 10^{-6} K^{-1}, \quad v_H = 0.29, \end{aligned} \tag{19}$$

in which $T = T_0 + \Delta T$ (K) and $T_0 = 300$ (K) is room temperature at which the sandwich panel is assumed to be thermal stress free. The CNTRC core is made of Poly (methyl methacrylate) matrix material, referred to as PMMA, and reinforced by (10, 10) single-walled carbon nanotubes (SWCNTs). The temperature dependent properties of the PMMA and (10, 10) SWCNTs can be found in many previous works, e.g. [4,7,18]. The CNT efficiency parameters given in the work [4] are $(\eta_1, \eta_2, \eta_3) = (0.137, 1.022, 0.715)$ for the case of $V^*_{CNT} = 0.12$, $(\eta_1, \eta_2, \eta_3) = (0.142, 1.626, 1.138)$ for the case of $V^*_{CNT} = 0.17$ and $(\eta_1, \eta_2, \eta_3) = (0.141, 1.585, 1.109)$ for the case of $V^*_{CNT} = 0.28$. In addition, it is assumed that $G_{13} = G_{12}$ and $G_{23} = 1.2G_{12}$ [4].

In numerical results, the effects of elastic foundations are evaluated by means of non-dimensional stiffness parameters defined as follows

$$(K_1, K_2) = \frac{b^2}{E_0^m h^3}\left(k_1 b^2, k_2\right), \tag{20}$$

in which E_0^m is the value of E^m computed at room temperature $T_0 = 300$ K. Furthermore, the degree of tangential restraints of boundary edges will be measured in a more convenient way by introducing the non-dimensional tangential stiffness parameters λ_1, λ_2 defined as follows

$$\lambda_1 = \frac{c_1}{c_1 + e_{11}}, \quad \lambda_2 = \frac{c_2}{c_2 + e_{11}}. \tag{21}$$

According to this definition, values of $\lambda_1 = 0$ (i.e. $c_1 = 0$), $\lambda_1 = 1$ (i.e. $c_1 \to \infty$) and $0 < \lambda_1 < 1$ ($0 < c_1 < \infty$) represent the cases of freely movable, fully immovable and partially movable edges $x = 0, a$, respectively. Similarly, movable, immovable and partially movable edges $y = 0, b$ are characterized by values of $\lambda_2 = 0, \lambda_2 = 1$ and $0 < \lambda_2 < 1$, respectively. Beside the commonly used value $K_S = 5/6$, another value of the shear correction coefficient is adopted in the present work as the following [30]

$$K_S = K_S^* = \frac{5}{6 - (\nu_{12}^{CNT} V^*_{CNT} + \nu^m V_m)}. \tag{22}$$

There is no investigation on the nonlinear stability of doubly curved sandwich panels with CNTRC core and tangentially restrained edges under external pressure in the literature. Therefore, to verify the proposed approach, comparative study is performed for special cases of geometry, material configuration and edge restraint, namely a FG-CNTRC cylindrical panel with movable edges, specialized from the present model for the cases of $R_x \to \infty$, $h_f = 0$ and $\lambda_1 = \lambda_2 = 0$.

Specifically, the load-deflection response of a FG-CNTRC cylindrical panel with movable edges under uniform external pressure at room temperature ($T = 300$ K) is traced using Eq. (18) and shown in Fig. 3 in comparison with result reported in the work of Shen and Xiang [7] making use of higher order shear deformation theory, asymptotic solutions and perturbation technique. In this comparison, CNTs are distributed according to FG-X pattern and $V^*_{CNT} = 0.28$. As can be seen, a good agreement is achieved in this comparison.

In what follows, the nonlinear stability of spherical and cylindrical sandwich panels with CNTRC core layer subjected to uniform external pressure will be analyzed. For the sake of brief expression, the panels are assumed to be geometrically perfect ($\mu = 0$), without foundation interactions ($K_1 = K_2 = 0$) and placed at room temperature ($T = 300$K), unless otherwise specified. It is found from Fig. 3 that results corresponding to $K_S = 5/6$ and $K_S = K_S^*$ are almost coincided. Accordingly, the following numerical illustrations are carried out for $K_S = K_S^*$.

The effects of CNT distribution in core layer on the nonlinear response of spherical sandwich panels with partially movable edges ($\lambda_1 = \lambda_2 = 0.5$) under uniform external pressure are analyzed in Fig. 4. It is evident that the load carrying capacity of the panel is the strongest when the CNTs are reinforced into core layer according to FG-X type. The positive efficiency of FG-X pattern of CNT distribution is more clear when the deflection of the panel is larger. Accordingly, the remaining analyses are carried out for sandwich panels with FG-X pattern of CNT distribution in the core layer. Subsequently, the load-deflection paths of spherical sandwich panels with partially restrained edges and various values of total volume fraction V_{CNT}^* of CNTs are depicted in Fig. 5. This figure demonstrates that the CNT reinforcements have positive influences on the load capacity of pressure-loaded sandwich panels with CNTRC core layer and load-deflection paths are significantly enhanced when the total volume fraction of CNTs is increased.

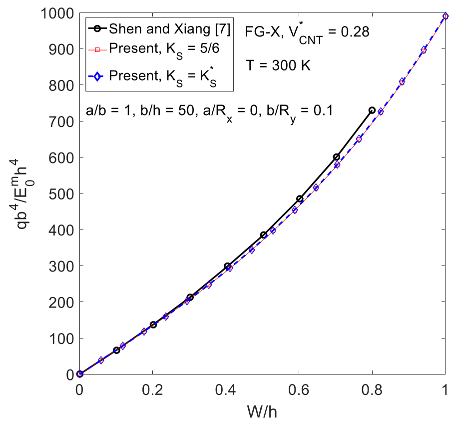

Fig. 3. Comparison of load-deflection response of FG-CNTRC cylindrical panel with movable edges under external pressure

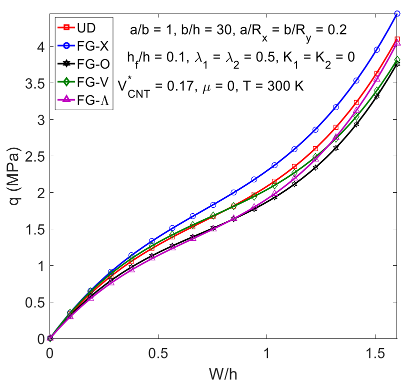

Fig. 4. Effects of CNT distribution pattern on load-deflection response of spherical sandwich panels under external pressure

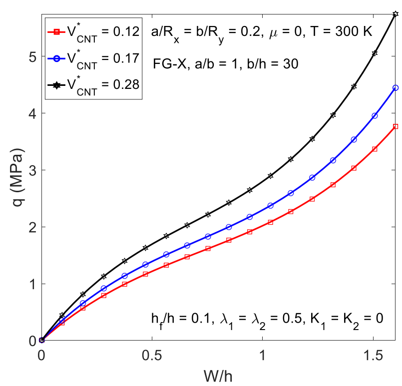

Fig. 5. Effects of CNT volume fraction on load-deflection response of spherical sandwich panels under external pressure

Subsequent numerical result is shown in Fig. 6 evaluating the effects of thickness of face sheet to total thickness h_f/h ratio on the load-deflection response of spherical sandwich panels under external pressure. It is realized that, for the considered material of face sheets, the load carrying capability of the panel is stronger when homogeneous face sheets become thicker. Next, the effects of various degrees of tangential constraints of boundary edges on the nonlinear stability of pressure-loaded spherical sandwich panels ($h_f/h = 0.15$, $V^*_{CNT} = 0.17$) are analyzed in Fig. 7. As can be seen, the load-deflection paths are significantly enhanced when tangential restraint parameters λ_1, λ_2 become larger, i.e. edges are more severely restrained. On the one hand, tangential restraints of edges have beneficial influences on the load carrying capability of pressure-loaded sandwich panels when the deflection is small. On the other hand, snap-through instability may occur when the edges are almost or fully immovable. In addition, it is recognized from Fig. 7 that equilibrium path of panel with $(\lambda_1, \lambda_2) = (0.5, 0)$ is remarkably higher than that of the panel with $(\lambda_1, \lambda_2) = (0, 0.5)$. This result reflects a fact that restraints of edges which are perpendicular and parallel to CNTs lead to significant and slight influences on the behavior tendency and load capacity of pressure-loaded sandwich panels, respectively.

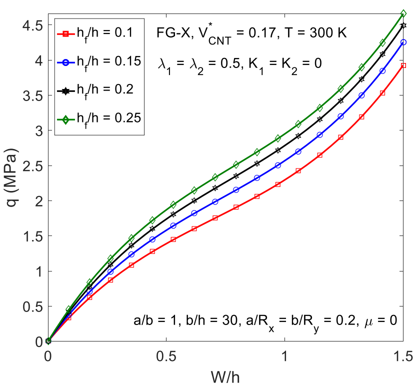

Fig. 6. Effects of thickness of face sheets on load-deflection response of spherical sandwich panels under external pressure

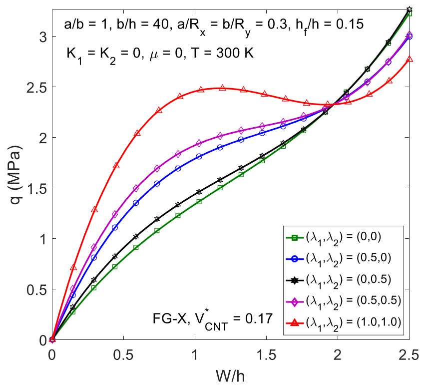

Fig. 7. Effects of tangential edge restraints on load-deflection response of spherical sandwich panels under external pressure

Subsequently, the effects of curvature ratios $a/R_x, b/R_y$ on the nonlinear stability of pressure-loaded curved sandwich panels with immovable edges ($\lambda_1 = \lambda_2 = 1$) are examined in Fig. 8. As can be observed, the equilibrium paths are higher when the curvature ratios become larger and, generally, spherical panel withstands external pressure better than cylindrical panel. It is similar to previous work of Shen and Xiang [15], snap-through instability can occur when curvature ratios $a/R_x, b/R_y$ become larger.

Furthermore, due to the anisotropy of CNTRC core layer, the effects of curvature in the x direction, i.e. a/R_x ratio, are more pronounced. Although equilibrium paths are higher in the region of small deflection, curved more sandwich panels may experience a limit-type buckling response accompanied by a snap-through instability in the postbuckling region.

In next illustration, the effects of elastic foundations on the nonlinear stability of spherical sandwich panels with immovable edges are sketched in Fig. 9. This figure

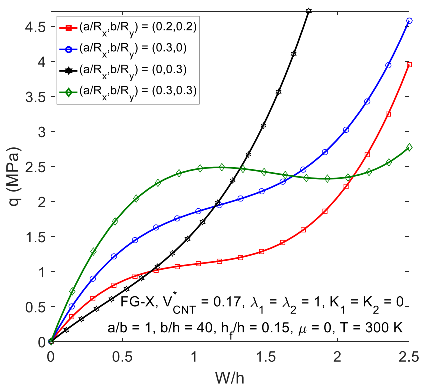

Fig. 8. Effects of curvature ratios on load-deflection response of curved sandwich panels under external pressure

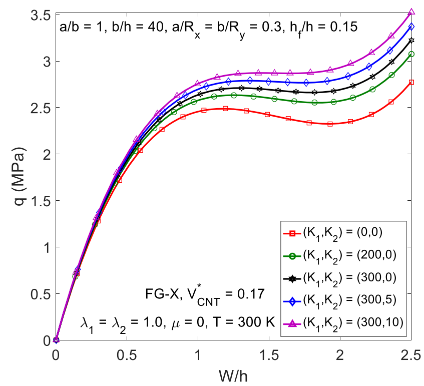

Fig. 9. Effects of elastic foundations on load-deflection response of spherical sandwich panels under external pressure

shows that elastic foundations have pronouncedly beneficial influences on the load carrying capability of the sandwich panels. More specifically, the snap-through instability of pressure-loaded curved sandwich panels can be alleviated or even eliminated by the support of elastic foundations, especially Winkler–Pasternak foundations.

Next, the effects of initial geometrical imperfection on the nonlinear stability of spherical sandwich panels with immovable edges resting on a Winkler–Pasternak foundation and subjected to external pressure are indicated in Fig. 10 in which positive and negative values of μ characterize inward and outward perturbations of the panels surfaces, respectively. Evidently, the imperfection has substantial influences on the behavior of pressure-loaded sandwich panels. Specifically, the equilibrium paths are lower and higher when the initial deviations of panel surfaces are inward and outward, respectively. Finally, the interactive influences of tangential edge constraints and elevated temperature on the nonlinear response of geometrically imperfect spherical sandwich panels on a Winkler

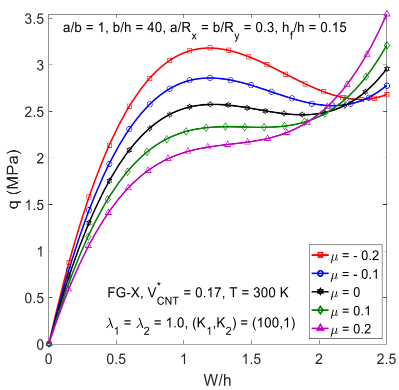

Fig. 10. Effects of geometrical imperfection on load-deflection response of spherical sandwich panels under external pressure

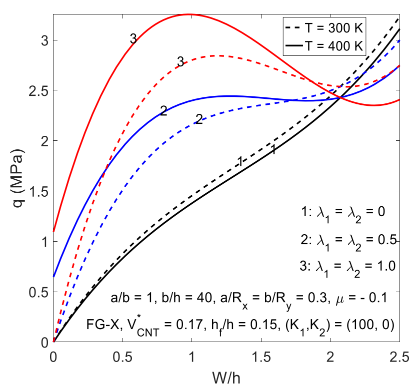

Fig. 11. Effects of tangential edge constraint and elevated temperature on load-deflection response of spherical sandwich panels

foundation are assessed in Fig. 11. When the edges are freely movable ($\lambda_1 = \lambda_2 = 0$), due to temperature dependence of material properties, the load capacity of pressure-loaded panels is decreased at elevated temperature ($T = 400$ K). In contrast, when the edges are tangentially restrained the pressure-loaded panels will exhibit a quasi-bifurcation response at elevated temperature. It can be explained that preexisting elevated temperature make the panel with restrained edges deflected outwards prior to applying external pressure and external pressure must reach a definite value for which the panel surfaces return initial geometry. It is also observed that load-deflection paths are higher and snap-through phenomenon is more intense when the edges are more rigorously restrained.

6. CONCLUDING REMARKS

The nonlinear stability response of doubly curved sandwich panels with FG-CNTRC core layer and tangentially restrained edges subjected to uniform external pressure in thermal environments has been investigated. From the above results, the following remarks are reached:

(1) The tangential constraints of boundary edges have dramatic influences on the nonlinear response and load carrying capacity of pressure-loaded sandwich panels. The load-deflection paths are higher and snap-through instability is possible when the edges are more rigorously restrained.

(2) Initial geometrical imperfection has significant effects on the effective curvature and load carrying capacity of the panel. Specifically, the inward and outward perturbations of the panel surfaces have deteriorative and beneficial influences on the stability of the panel, respectively.

(3) Unlike case of movable edges, preexisting elevated temperature has substantial influences on the behavior tendency and load carrying capability of curved sandwich panels with restrained edges under external pressure. When the edges are restrained, pressure-loaded sandwich panels can exhibit a quasi-bifurcation response at elevated temperature.

ACKNOWLEDGMENT

This research is funded by Vietnam National Foundation for Science and Technology Development (NAFOSTED) under grant number 107.02-2019.318.

REFERENCES

[1] E. T. Thostenson, Z. Ren, and T.-W. Chou. Advances in the science and technology of carbon nanotubes and their composites: a review. *Composites Science and Technology*, **61**, (2001), pp. 1899–1912. https://doi.org/10.1016/s0266-3538(01)00094-x.

[2] J. N. Coleman, U. Khan, W. J. Blau, and Y. K. Gun'ko. Small but strong: A review of the mechanical properties of carbon nanotube–polymer composites. *Carbon*, **44**, (2006), pp. 1624–1652. https://doi.org/10.1016/j.carbon.2006.02.038.

[3] H.-S. Shen. Nonlinear bending of functionally graded carbon nanotube-reinforced composite plates in thermal environments. *Composite Structures*, **91**, (2009), pp. 9–19. https://doi.org/10.1016/j.compstruct.2009.04.026.

[4] H.-S. Shen and C.-L. Zhang. Thermal buckling and postbuckling behavior of functionally graded carbon nanotube-reinforced composite plates. *Materials & Design*, **31**, (2010), pp. 3403–3411. https://doi.org/10.1016/j.matdes.2010.01.048.

[5] H.-S. Shen. Postbuckling of nanotube-reinforced composite cylindrical panels resting on elastic foundations subjected to lateral pressure in thermal environments. *Engineering Structures*, **122**, (2016), pp. 174–183. https://doi.org/10.1016/j.engstruct.2016.05.004.

[6] H.-S. Shen and Y. Xiang. Postbuckling of axially compressed nanotube-reinforced composite cylindrical panels resting on elastic foundations in thermal environments. *Composites Part B: Engineering*, **67**, (2014), pp. 50–61. https://doi.org/10.1016/j.compositesb.2014.06.020.

[7] H.-S. Shen and Y. Xiang. Nonlinear bending of nanotube-reinforced composite cylindrical panels resting on elastic foundations in thermal environments. *Engineering Structures*, **80**, (2014), pp. 163–172. https://doi.org/10.1016/j.engstruct.2014.08.038.

[8] H. V. Tung and L. T. N. Trang. Thermal postbuckling of shear deformable CNT-reinforced composite plates with tangentially restrained edges and temperature-dependent properties. *Journal of Thermoplastic Composite Materials*, **33**, (2018), pp. 97–124. https://doi.org/10.1177/0892705718804588.

[9] L. T. N. Trang and H. V. Tung. Thermomechanical nonlinear stability of pressure-loaded CNT-reinforced composite doubly curved panels resting on elastic foundations. *Nonlinear Engineering*, **8**, (2019), pp. 582–596. https://doi.org/10.1515/nleng-2018-0077.

[10] L. T. N. Trang and H. V. Tung. Thermomechanical nonlinear stability of pressure-loaded functionally graded carbon nanotube-reinforced composite doubly curved panels with tangentially restrained edges. *Proceedings of the Institution of Mechanical Engineers, Part C: Journal of Mechanical Engineering Science*, **233**, (2019), pp. 5848–5859. https://doi.org/10.1177/0954406219856374.

[11] H. V. Tung and P. T. Hieu. Nonlinear buckling of CNT-reinforced composite toroidal shell segment surrounded by an elastic medium and subjected to uniform external pressure. *Vietnam Journal of Mechanics*, **40**, (2018), pp. 285–301. https://doi.org/10.15625/0866-7136/12397.

[12] P. T. Hieu and H. V. Tung. Thermomechanical nonlinear buckling of pressure-loaded carbon nanotube reinforced composite toroidal shell segment surrounded by an elastic medium with tangentially restrained edges. *Proceedings of the Institution of Mechanical Engineers, Part C: Journal of Mechanical Engineering Science*, **233**, (2018), pp. 3193–3207. https://doi.org/10.1177/0954406218802942.

[13] P. T. Hieu and H. V. Tung. Thermomechanical postbuckling of pressure-loaded CNT-reinforced composite cylindrical shells under tangential edge constraints and various temperature conditions. *Polymer Composites*, **41**, (2019), pp. 244–257. https://doi.org/10.1002/pc.25365.

[14] H.-S. Shen, J. N. Reddy, and Y. Yu. Postbuckling of doubly curved FG-GRC laminated panels subjected to lateral pressure in thermal environments. *Mechanics of Advanced Materials and Structures*, **28**, (2019), pp. 260–270. https://doi.org/10.1080/15376494.2018.1556827.

[15] H.-S. Shen and Y. Xiang. Postbuckling of pressure-loaded nanotube-reinforced composite doubly curved panels resting on elastic foundations in thermal environments. *International Journal of Mechanical Sciences*, **107**, (2016), pp. 225–234. https://doi.org/10.1016/j.ijmecsci.2016.01.004.

[16] H.-S. Shen and H. Wang. Postbuckling of pressure-loaded FGM doubly curved panels resting on elastic foundations in thermal environments. *Thin-Walled Structures*, **100**, (2016), pp. 124–133. https://doi.org/10.1016/j.tws.2015.11.015.

[17] H.-S. Shen and Z. H. Zhu. Postbuckling of sandwich plates with nanotube-reinforced composite face sheets resting on elastic foundations. *European Journal of Mechanics - A/Solids*, **35**, (2012), pp. 10–21. https://doi.org/10.1016/j.euromechsol.2012.01.005.
[18] Y. Kiani. Thermal post-buckling of temperature dependent sandwich plates with FG-CNTRC face sheets. *Journal of Thermal Stresses*, **41**, (2018), pp. 866–882. https://doi.org/10.1080/01495739.2018.1425645.
[19] K. Mehar, S. K. Panda, and T. R. Mahapatra. Nonlinear frequency responses of functionally graded carbon nanotube-reinforced sandwich curved panel under uniform temperature field. *International Journal of Applied Mechanics*, **10**, (2018), p. 1850028. https://doi.org/10.1142/s175882511850028x.
[20] K. Mehar and S. K. Panda. Thermal free vibration behavior of FG-CNT reinforced sandwich curved panel using finite element method. *Polymer Composites*, **39**, (2017), pp. 2751–2764. https://doi.org/10.1002/pc.24266.
[21] K. Mehar, S. K. Panda, Y. Devarajan, and G. Choubey. Numerical buckling analysis of graded CNT-reinforced composite sandwich shell structure under thermal loading. *Composite Structures*, **216**, (2019), pp. 406–414. https://doi.org/10.1016/j.compstruct.2019.03.002.
[22] A. Sankar, S. Natarajan, T. B. Zineb, and M. Ganapathi. Investigation of supersonic flutter of thick doubly curved sandwich panels with CNT reinforced facesheets using higher-order structural theory. *Composite Structures*, **127**, (2015), pp. 340–355. https://doi.org/10.1016/j.compstruct.2015.02.047.
[23] M. Wang, Z.-M. Li, and P. Qiao. Vibration analysis of sandwich plates with carbon nanotube-reinforced composite face-sheets. *Composite Structures*, **200**, (2018), pp. 799–809. https://doi.org/10.1016/j.compstruct.2018.05.058.
[24] V. T. Long and H. V. Tung. Thermal postbuckling behavior of CNT-reinforced composite sandwich plate models resting on elastic foundations with tangentially restrained edges and temperature-dependent properties. *Journal of Thermoplastic Composite Materials*, **33**, (2019), pp. 1396–1428. https://doi.org/10.1177/0892705719828789.
[25] V. T. Long and H. V. Tung. Thermomechanical postbuckling behavior of CNT-reinforced composite sandwich plate models resting on elastic foundations with elastically restrained unloaded edges. *Journal of Thermal Stresses*, **42**, (2019), pp. 658–680. https://doi.org/10.1080/01495739.2019.1571972.
[26] H. V. Tung and V. T. Long. Buckling and postbuckling of CNT-reinforced composite sandwich cylindrical panels subjected to axial compression in thermal environments. *Vietnam Journal of Mechanics*, **41**, (2019), pp. 217–231. https://doi.org/10.15625/0866-7136/13673.
[27] H. V. Tung and P. T. Hieu. Thermal and thermomechanical buckling of CNT-reinforced composite sandwich cylindrical shells including elasticity of tangential edge restraint. *Vietnam Journal of Mechanics*, (2021). https://doi.org/10.15625/0866-7136/16118.
[28] K. Foroutan, E. Carrera, and H. Ahmadi. Static and dynamic hygrothermal postbuckling analysis of sandwich cylindrical panels with an FG-CNTRC core surrounded by nonlinear viscoelastic foundations. *Composite Structures*, **259**, (2021), p. 113214. https://doi.org/10.1016/j.compstruct.2020.113214.
[29] J. N. Reddy. *Mechanics of laminated composite plates and shells: Theory and Analysis*. CRC Press, (2004). https://doi.org/10.1201/b12409.
[30] E. Efraim and M. Eisenberger. Exact vibration analysis of variable thickness thick annular isotropic and FGM plates. *Journal of Sound and Vibration*, **299**, (2007), pp. 720–738. https://doi.org/10.1016/j.jsv.2006.06.068.